
Single Person Pose Estimation: A Survey

Feng Zhang · Xiatian Zhu · Chen Wang

Abstract Human pose estimation in unconstrained images and videos is a fundamental computer vision task. To illustrate the evolutionary path in technique, in this survey we summarize representative human pose methods in a structured taxonomy, with a particular focus on deep learning models and single-person image setting. Specifically, we examine and survey all the components of a typical human pose estimation pipeline, including *data augmentation, model architecture and backbone, supervision representation, post-processing, standard datasets, evaluation metrics*. To envisage the future directions, we finally discuss the key unsolved problems and potential trends for human pose estimation.

Keywords Human pose estimation · Single person · Deep learning · Survey

1 Introduction

Human Pose Estimation (HPE) is a fundamental problem in computer vision. HPE aims to obtain the spatial coordinates of human body joints in a person image, with a wide variety of applications such as action recognition [92], person re-identification [94], semantic segmentation [42], human-robot interaction [83], etc. It

is challenging due to heavy occlusions, varying clothing styles, poor lighting conditions and various shooting angles. Earlier HPE methods [30, 27, 1, 88, 39] adopt hand-crafted features to describe human body. Mostly, these methods aim to learn the underlying relations between different body parts, e.g., using the seminal pictorial structure model [30]. However, they are limited in accuracy especially under severe occlusions and complex lighting conditions, partly due to less expressive representations.

In the past years, inspired by the great success of deep learning in image recognition [41] characterized by end-to-end feature learning capability, researchers have introduced an increasing number of deep human pose models [76, 80, 52, 82, 70] and continuously refresh the state-of-the-art model performance on standard data benchmarks. Deep learning based human pose estimation has become a more exciting and active research area since the first introduction of deep learning in 2014 [76]. Given the large body of deep human pose estimation works published thus far, we consider that it is time to review this field for three main purposes: (1) To reflect its development trajectory and process by extensively surveying previous methods and algorithms; (2) To structure different classes of human pose methods; (3) To provide a holistic picture and schematic overview of the whole field. These are not only useful and informative for the beginners to understand quickly the current state-of-the-art methods for human pose estimation, but also indicative and inspiring for the experts to further push the forefront edges.

There exist a number of surveys on human pose estimation in the literature [37, 48, 32, 65, 78, 24, 17]. However, most of existing surveys [65, 78, 37, 24] focus on basic foundations and knowledge, without comprehensive review on deep learning human pose estimation methods. Whilst [48, 32] focus on reviewing human pose

Feng Zhang
School of Computer Science and Technology, Nanjing University of Posts and Telecommunications, Nanjing, China. E-mail: zhangfeng.ac@outlook.com
Xiatian Zhu
Centre for Vision, Speech and Signal Processing, University of Surrey, Guildford GU2 7XH, United Kingdom. E-mail: eddy.zhuxt@gmail.com
Chen Wang
School of Computer Science and Engineering, University of Electronic Science and Technology of China, Chengdu, China. E-mail: wangchen199179@gmail.com

methods, they are largely out-of-date with a high desire for covering the latest research advances. This survey timely solves this need with focus on deep learning based human pose estimation on single-person images in particular. This is because multi-person human pose estimation can be easily decomposed into person detection and pose estimation, which represents the state-of-the-art solutions [76, 80, 52, 82, 70].

1.1 Overview

To organize a large number of existing deep learning HPE methods in an intuitive manner, we propose a novel taxonomy from the model component perspective. Table 1 show our proposed taxonomy with a system pipeline illustrated in Fig. 1. Accordingly, our survey is organized as the following: Section 2 describes the common data augmentation strategies that are important for boosting the model performance. Section 3 presents typical model architectures and network backbones. Section 4 reviews the largely ignored yet significant post-processing. Section 5 details the supervision representation used in optimization. Section 6 and Section 7 summarize the standard human pose datasets and performance evaluation metrics, respectively.

2 Data Augmentation

As a generic and common model training strategy, data augmentation is critical for the generalization performance of deep learning methods including human pose models, due to the data hungry nature of deep neural networks [23, 41, 67] and the difficulty of collecting large training data. Often it is considered as a regularization which can mitigate the notorious overfitting problem. In general, data augmentation would generate more training samples by introducing some modification to the original training data whilst keeping the same semantic labels. There are random and optimized data augmentation for training human pose models, as detailed below.

2.1 Random Data Augmentation

Data augmentation operations are often randomly applied to a training sample during training. The common augmentation operations include flipping, rotating, scaling, occluding, and color jittering [59].

Flipping. Flipping can improve the model’s robustness against imaging direction. There are two types of flipping: horizontal flipping and vertical flipping. Horizontal flipping is used more than the vertical one. In model training, the flipping augmentation is usually triggered at a certain probability, e.g. 50%.

Rotation. Human bodies may be lying and leaning with the body spines exhibiting different angles in imbalanced distribution. This imbalance may impose negative effect to model training. Rotation augmentation is a simple solution for mitigating this. It is performed by rotating the image clockwise or counterclockwise around the center of human body. Typically, the rotation angle ranges from -30 to 30 degrees. As flipping, the rotation operation is also triggered at a preset probability.

Scaling. Body scale variation is often large in unconstrained images which might negatively affect the performance of human pose estimation methods. To alleviate this issue, scaling augmentation is adopted to improve the model robustness for image scales. In training, a random scaling factor is selected and applied.

Color jittering. Human person images are typically collected in a variety of environments with different lighting conditions. To make the model suitable to cope with such image data, color jittering is effective to simulate diverse lighting conditions in training.

Occlusion. Occlusion is an inevitable challenge due to uncontrolled shooting angle and complex scene. Excepted collecting samples which is largely limited, synthesizing images with occlusions turns out to be cheaper and easier for improving model training.

Pose-specific augmentations. All the above augmentation operations are generally applicable for many different computer vision tasks. Besides, pose-specific augmentation techniques [40, 79, 57] have been proposed additionally. Specifically, in the real world, it is often the case that human body joints are obscured by other objects; In crowded scenes, there may be multiple joints of the same class that can greatly confuse a model. Under such observation, Ke et al. [40] proposed a keypoint-masking augmentation method to synthesize hard training samples with self-occlusion and mutual interference. Considering that there are a large number of samples with a certain part of human body and the upper body presents easier-to-detect joints than the

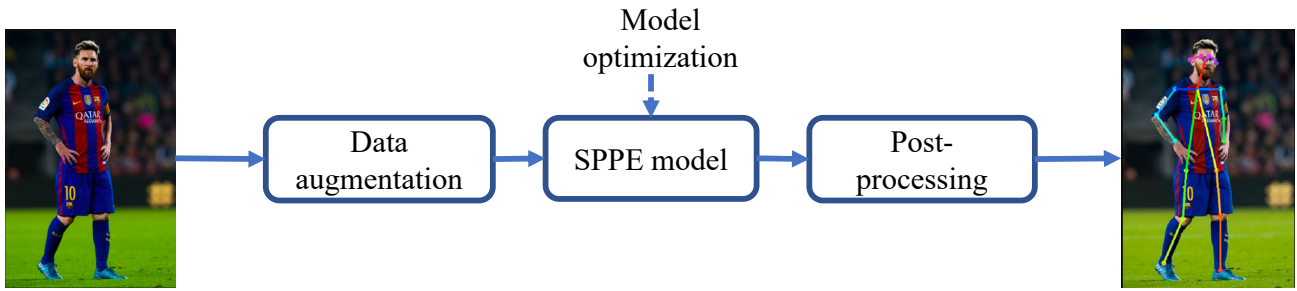


Fig. 1 The deep learning pipeline of human pose estimation in the single-person setting.

Table 1 The taxonomy of human pose estimation in the model component perspective.

Perspective	Category	Sub-category
Data augmentation	Random data augmentation	Generic data augmentation [75, 60]
		Pose-specific data augmentation [40, 79, 57]
	Optimized data augmentation	Neural Architecture Search (NAS) based methods [35]
		Generative Adversarial Network (GAN) based methods [58]
Deep human pose model	Model architecture	Sequential architectures [36, 26, 60, 62, 54, 70, 73, 68]
		Cascaded architectures [76, 74, 80, 69, 52, 87, 40, 16, 46, 55, 91]
		Recurrent architectures [60, 5, 10, 31]
		Adversarial architectures [15, 19]
		Neural Architecture Search (NAS) [95, 4, 44, 85, 33]
	Network design	Multi-scale feature learning [74, 52, 87, 55, 46, 16, 9, 70, 68, 3]
		Prior knowledge incorporation [55, 8, 81, 54]
		Spatial relation modelling [14, 75, 86, 21, 20, 71, 43, 15, 73, 91]
Attention mechanism [22, 46, 68]		
Supervision representation	Heatmap based methods	Heatmap regression [75, 60, 80, 46, 70]
		Heatmap regression and offset regression [56]
	Coordinate based methods	Direct coordinate regression [76, 26, 69]
		Coordinate regression through heatmap [72]
Post-processing	Heuristic methods	Empirical design [52]
	Data-driven methods	Distribution learning [90, 84]

lower body, Wang et al. [79] presented a half-body augmentation strategy for more specific operation. It is observed that samples with few keypoints in the training set are corner cases often simply ignored by existing methods. To better solve this problem, Park et al. [57] introduced a body-part-cropping augmentation approach by randomly selecting and cropping a proportion of human body at different scales to increase the diversity of training data.

2.2 Optimized Data Augmentation

Random data augmentation is simple yet less efficient. This can be addressed by learning to augment training data, i.e., optimized data augmentation. It is a relatively new research direction in human pose estimation. Two representative types of learning framework in the literature are *adversarial learning* and *neural architecture search*.

The first type usually employs the generative adversarial networks (GANs). The key idea is to generate *hard training samples* that can more effectively incur training loss and therefore expedite model learning. For example, Peng et al. [58] proposed Online Adversarial Augmentation Network (OAAN) jointly learned with an existing HPE model. OAAN is designed to generate hard adversarial samples with a reward-penalty policy in a way that the target HPE model can improve its robustness against hard samples. Bin et al. [6] proposed a Semantic Data Augmentation (SDA) method. It aims to solve the limitation of random data augmentation [40] that generated samples by a naive copying-and-pasting body part strategy have limited diversity and unrealistic appearance. SDA involves constructing semantic body part pool for generation of hard training samples. Specifically, a semantic body part pool is first constructed by a human parsing algorithm; Then, hard training samples are generated with an optimal pasting configuration in an adversarial learning manner.

Unlike adversarial learning based methods, the second type instead aims to optimize the data augmentation application process. For instance, Hou et al. [35] first defined a search space with different operators such as flipping, cropping, rotation. By treating the sequence of applying these operators as a trainable component, they turned this problem into a discrete optimization problem and solved it via an existing differentiable search algorithm [45].

3 Model Architecture and Network Design

According to the theory that the structure of neural networks determines its function, the human brain has highly structured connections at birth which determines what functions it has. These functions in the brain are enhanced through learning subsequently. Like these networks in the brain, their architectures and backbones play a very important role in HPE. How to design a good architecture and backbone encoding human prior knowledge remains an open problem. The models taking the scale variability and severe occlusions into consideration make it possible to learn the complex mapping from natural image to body pose. This section will describe the recent researches of the HPE model from the two perspectives: the architecture and backbone.

3.1 Model Architecture

The architecture of HPE model can be classified into four categories: sequential, cascaded, recurrent and adversarial architectures.

(I) Sequential architecture. Typical sequential models [36, 26, 60, 62, 54, 70, 73, 68] construct a simple yet intuitive framework by a series of basic layers such as convolution, pooling, fully connection to learn a mapping from input images to joint coordinates. Jain et al. [36] proposed a CNN architecture with fully connected layers. The network slides over the input image with an overlapped sliding window to detect the presence of joints. Fan et al. [26] developed a dual-source network architecture that uses the raw image with a holistic view and the image patches with a local view as model inputs to improve the accuracy of HPE.

To avoid kinematically impossible predictions, Pfister et al. [60] presented a novel architecture that includes a spatial fusion layer to learn spatial dependencies of joints implicitly. Rafi et al. [62] adopted an efficient multi-scale network architecture based on the Inception network to reduce the model complexity and improve the model’s ability to perceive larger context. Nie et al. [54] proposed the Parsing Induced Learner (PIL) method to facilitate the HPE model with parsing information. Sun et al. [70] proposed a network architecture that preserves high-resolution features and fused low-resolution features with high-resolution features to learn robust multi-scale feature representations.

Previous HPE models learn the shared feature representations for all body parts, Tang et al. [73] found that the shared feature representations are beneficial to related parts but fail to improve the learning of other parts. To address this problem, they obtained the correlations between joints through statistical analysis and designed a sequential network architecture with multiple branches to incorporate structured knowledge of human body into the network architecture design. Su et al. [68] designed the Channel Shuffle Module (CSM) and the Spatial Channel-wise Attention Residual Bottleneck (SCARB) to introduce the attention mechanism into the networks. Specifically, the CSM can improve the information exchange across channels and the SCARB is able to boost the residual learning. Inspired by the Atrous Spatial Pyramid Pooling (ASPP) in semantic segmentation, Artacho et al. [3] proposed the Waterfall Atrous Spatial Pooling (WASP) module to enlarge the Field of View (FOV) and obtain multi-scale representations.

(II) Cascaded architecture. The cascaded architecture usually repeats several modules to refine the

prediction. Toshev et al. [76] presented the first application of CNNs to human pose estimation and designed a cascaded architecture. The regressor in the first stage aims at estimating coarse body pose and the subsequent regressors are designed to learn the displacement of the part locations from the previous stage to the ground-truth locations.

Traditional architectures for classification use down-sampling layers such as pooling to maintain invariance, reduce computation and improve efficiency, but these pooling layers in the network are not appropriate for the HPE task and may hurt the model performance. Thompson et al. [74] reduced the number of down-sampling layers and implemented a sliding-window detector with overlapping contexts to produce coarse predictions and then used the Siamese network to refine these coarse locations. Wei et al. [80] designed a multi-stage architecture called Convolutional Pose Machine (CPM) to learn long-range dependencies between joints. The CPM consists of several stages and each stage operates on the predicted heatmaps from the previous stage. The spatial relations of joints are captured through increasing the size of receptive field for each subnetwork in the CPM. Sun et al. [69] analyzed the relative locations of joints and found the uniform distribution of these relative locations has a negative effect on the learning procedure. To make the learning procedure easier, they proposed a novel network with normalization module which is composed of body normalization and limb normalization.

To extract multi-scale features and deal with ambiguous prediction, Newell et al. [52] designed the hourglass module by repeating the bottom-up and top-down processing. Yang et al. [87] introduced the fractional pooling into the residual block and proposed the Pyramid Residual Module (PRM) to learn scale-invariant representations from training data. Ke et al. [40] proposed a multi-scale structure learning framework based on the revised hourglass module and utilized additional multi-scale regression to perform global optimization of structure configuration. There are occluded joints, invisible joints, and very complex backgrounds in the real world. To cope with these challenging cases, Chen et al. [16] proposed a novel network structure called Cascaded Pyramid Network (CPN) consisting of a GlobalNet and a RefineNet. The GlobalNet is responsible for the easy samples and the RefineNet aims at dealing with those challenging samples. Liu et al. [46] designed a Cascaded Inception of Inception Network (CIOIN). The Inception of Inception (IOI) block in CIOIN is able to fuse features with different semantics and preserve the scale diversity in them. The Attention-modulated IOI (AIOI) block is capable of adjusting the importance

of features according to the context. The CIOIN architecture employs a multiple iterative stage to capture long-range dependencies. Ning et al. [55] constructed a fractal network by using the hourglass modules and Inception-ResNet blocks to regress human pose without explicit graphical modelling. To extract contextual information, Zhang et al. [91] proposed the Cascade Prediction Fusion (CPF) to fuse predictions and features from the previous stage. To learn relations between joints, they further designed the Pose Graph Neural Network (PGNN) to model these relations according to the body structure.

(III) Recurrent architecture. Feedforward architectures are able to learn hierarchical feature representations from data, but they fail to capture the connections between joints and the associations between features from different layers. Recurrent architectures enhance the feature representations and incorporate top-down feedback into the feedforward architectures to complement their feature representations, establishing relations between the input space and the output space. Pfister et al. [60] made the first attempt to model features from different layers by leveraging the proposed spatial fusion layer. Inspired by Pfister, Belagiannis et al. [5] presented a novel recurrent model including a feedforward module and several recurrent modules. These recurrent modules can effectively revise predictions with iterative feature fusion. Carreira et al. [10] implemented a self-correction model which simulates the recurrent mechanism in the human brain to learn a residual displacement from current prediction to the ground truth progressively in an Iterative Error Feedback (IEF) manner. Unlike previous studies [60, 5, 10] on recurrent architecture, Gkioxari et al. [31] defined a fixed ordering of joints based on the kinematic tree of the human body and modelled the dependencies between adjacent joints by learning a conditional distribution to predict joints one by one.

(IV) Adversarial architecture. GAN consists of a generator and a discriminator, and is trained by playing minimax game between the generator and the discriminator. The generator synthesizes samples capable of confusing the discriminator, while the discriminator continuously improves its capability in distinguishing fake samples from the true data distribution. Recent applications of GAN in human pose estimation include [15] and [19] view the generator as a HPE network. They treat the discriminator as a proxy of the loss function to guide the learning process of the generator by imposing geometric constraints and prior knowledge through the discriminator. To exploit body configurations and enforce structure constraints on HPE

model, Chen et al. [15] developed two discriminators (a pose discriminator and a confidence discriminator). The pose discriminator is responsible for identifying whether the locations of joints estimated by the generator are reasonable or not, and the confidence discriminator can utilize the geometric structure of the human body to evaluate these predictions with high confidence, especially the occluded joints with high confidence. Different from [15], Chou et al. [19] proposed a discriminator to reconstruct heatmaps. For j -th joint, the discriminator is optimized by minimizing the loss L_{fake} between the generated heatmaps $\{\hat{C}_j\}_{j=1}^J$ and the reconstructed ones $\{D(\hat{C}_j, X)\}_{j=1}^J$ (Eq.(2)), and it tries to maximize the loss L_{real} between the ground-truth heatmaps $\{C_j\}_{j=1}^J$ and the reconstructed ones $\{D(C_j, X)\}_{j=1}^J$ (Eq.(1)).

$$L_{real} = \sum_{j=1}^M (C_j - D(C_j, X))^2 \quad (1)$$

$$L_{fake} = \sum_{j=1}^M (\hat{C}_j - D(\hat{C}_j, X))^2 \quad (2)$$

Neural architecture search. In practice, the hand-designed architecture needs to be adjusted according to the requirements of a specific task. However, these modifications involve tedious verification process. Therefore, Neural Architecture Search (NAS) is presented to find good network architecture with limited computing resources and little human intervention. Zoph et al. [95] and Baker et al. [4] introduced Reinforcement Learning (RL) into NAS by modelling the searching process as a Markov Decision Process (MDP). However, this kind of methods consume too many computing resources making them infeasible to practical applications.

In order to reduce the search time, Liu et al. [44] proposed the DARTs method which implements a continuous relaxed representation of the architecture. Specifically, they replaced the discrete non-differentiable search space in RL based approaches to obtain the optimal architecture by gradient descent efficiently. Motivated by Convolutional Neural Fabrics [66] and DARTS [44], Yang et al. [85] designed the part representation according to the structure of human skeleton and parameterized the Cell-based Neural Fabric (CNF) to perform the gradient-based search at the micro and macro search space. Gong et al. [33] presented a novel NAS framework called AutoPose which defines a hierarchical multi-scale search space and utilizes both gradient-based cell-level search and reinforcement learning based network-level search to discover multiple parallel branches of diverse scales.

3.2 Network Design

Multi-scale feature learning. The main purpose of the research of HPE is to extract multi-scale features to cope with various scales of the human body and to obtain a larger receptive field for global inference. Tompson et al. [74] proposed a two-stage network with pose refinement implemented by a Siamese network. The Siamese network takes the coarse heatmaps with different resolutions as inputs to refine predictions.

To handle body parts with different scales such as the face, hand, foot, etc, Newell et al. [52] presented the stacked hourglass network formed by stacking several hourglass modules with pooling and upsampling operations to capture features at every scale. Motivated by the residual learning [34], Wei et al. [87] proposed several variants of Pyramid Residual Modules (PRMs) simulating the mechanism of human visual perception to capture multi-scale features. Ning et al. [55] adopted the design of Inception block and residual block, and proposed the Inception-ResNet module to construct a fractal network structure which captures the interdependence between joints across different scales and resolutions.

To deal with various appearance and occlusion in human pose estimation, Liu et al. [46] proposed a Cascaded Inception of Inception Network (CIOIN). The Inception of Inception (IOI) block in the CIOIN not only is able to preserve scale diversity but also can be upgraded to the Attention-modulated IOI (AIOI) block to reweight the features with different scales. Chen et al. [16] designed the Cascaded Pyramid Network (CPN) architecture based on the ResNet backbone, and they integrated the U-shape structure into the architecture design to create a feature pyramid that is able to preserve spatial information of multi-scale features. Cao et al. [9] introduced a stronger low-level feature module called Feature Pyramid Stem (FPS). The FPS module is capable of extracting target-specific features in valid regions, and progressively fusing features with different resolutions to improve the quality of representations.

Most of the existing architectures utilize the high-to-low and low-to-high process to learn the multi-scale feature representations. However, recovering from low-resolution representations does not bring more useful information. How to maintain high-resolution and multi-scale representations is a non-negligible concern in architecture design. Sun et al. [70] presented a novel architecture, namely HighResolution Net (HRNet), which can maintain high-resolution representations through the whole process. Su et al. [68] proposed a Channel Shuffle Module (CSM) to further enhance the cross-

channel information exchange between feature maps with different scales.

To exploit the contextual information, enlarge the field-of-view, and enhance multi-scale representations, Artacho et al. [3] proposed the Waterfall Atrous Spatial Pooling (WASP) module. The WASP module employs cascaded atrous convolutions at increasing rates in the parallel architecture to obtain larger field-of-view.

Prior knowledge incorporation. Although end-to-end networks can learn discriminative feature representations, the HPE model trained from limited data cannot describe the actual distribution. How to encode prior knowledge into neural networks is a very complicated task. To solve this problem, Ning et al. [55] designed two types of external knowledge that includes geometrical features and Histogram of Gradients (HOG) based features. They utilized the proposed knowledge projection module to decode the abstract external knowledge and injected the decoded knowledge into the fractal network. Bulat et al. [8] proposed a part detection network to capture contextual information and structured relations. The part detection network guides the pose regression network to learn the structure of body parts, improving the predictions of occluded parts with low confidence scores.

Motivated by the correlations between part segmentation and pose estimation, Xia et al. [81] proposed a prior knowledge incorporation schema to exploit segmentation results to improve HPE. Specifically, semantic part prior knowledge from part Fully Convolutional Network (FCN) is fed to Fully-connected Conditional Random Field (FCRF) to avoid unreasonable predictions from the pose FCN. Nie et al. [54] proposed a parsing-guided HPE method which uses the Parsing Induced Learner (PIL) to learn the parameters of adaptive convolution from the features of the parsing encoder. Specifically, they leverages the adaptive convolution to adjust features from the pose encoder to obtain accurate predictions.

Spatial relation modelling. The dimension of input space is determined by many factors such as deformation caused by the varying viewing angles, changes in lighting and clothing, and occlusion induced by human-object interaction. The mapping from image to pose is highly non-linear, which makes it necessary to exploit the spatial inter-dependencies between joints to improve the representation ability of HPE model. Chen et al. [14] defined a tree-structure graphic model to learn spatial relations by conditional probabilities from unary term and Image Dependent Pairwise Relationships (IDPR) term, and adopted Dynamic Programming (DP) algorithm to find the optimal configuration

for person instances. Tompson et al. [75] proposed a Markov Random Field (MRF) model which contains a unary term for modelling joint locations and a pairwise term for modelling the conditional distribution of neighbouring joints. They implemented the MRF model by the message passing network to eliminate incorrect predictions.

Different from the MRF-liked model [75], Yang et al. [86] blended the appearance mixtures into the loopy model to enforce deformation constraints, which allows the HPE model to handle large pose variations. Instead of modelling structures by graphical models [75, 86, 21], Chu et al. [21] proposed a CRF-CNN framework which extends the loopy model by adding a novel pairwise term to learn the relations and structures among features. To refine feature maps, Chu et al. [20] presented a bi-directional structured feature learning model by utilizing geometrical transform kernels to pass on information between feature maps for each joint. Sun et al. [71] introduced an intuitive yet stable bone-based representation which is easier to learn and more stable than traditional joint-based representation to encode the inter-dependencies inside the structure of body pose. Lifshitz et al. [43] designed a voting representation by log-polar binning and then aggregated voting maps using a large deconvolution kernel. They added a novel image-based consensus voting binary term to remove the independence assumption in traditional binary term by averaging over all locations in the voting maps.

Motivated by the GAN, Chen et al. [15] proposed a pose discriminator which implicitly exploits the spatial inter-relations of joints to distinguish the fake poses from the real ones. Tang et al. [73] analyzed the correlations between different body parts, and obtained related parts by applying spectral clustering to the correlation matrix. They designed a part-based branching network according to the compositionality of human bodies to learn specific high-level features for better performance.

Graphical models involving multiple sequential updates usually incur accumulative error. Instead of defining an explicit graphical model to learn the structure of the human body, Zhang et al. [91] integrated Pose Graph Neural Network (PGNN) into the HPE network to exploit spatial contextual information from neighbouring joints.

Attention mechanism. Attention mechanism in the human visual system helps the brain ignore irrelevant regions and pay more attention to important information. In the field of HPE, attention mechanism can also be integrated into existing networks to help HPE mod-

els focus on relevant areas. Chu et al. [22] designed three types of attention modules for HPE. The multi-resolution attention within the hourglass module aims to refine features, and the multi-semantics attention across several stacks of hourglass is used to capture various semantic information. Besides, the hierarchical attention is adopted to encode holistic and local body structure. Liu et al. [46] introduced an Inception of Inception (IOI) module to preserve low-level features. To improve the robustness of the HPE model against scale variety, they incorporated the attention mechanism into the IOI module to form an Attention-modulated IOI (AIOI) module to fuse multi-scale features dynamically. To learn the relations between the low-level and high-level feature maps, Su et al. [68] proposed a Channel Shuffle Module (CSM) implemented by channel shuffle operation to exchange information within feature pyramid, and designed a Spatial Channel-wise Attention Residual Bottleneck (SCARB) to highlight the spatial and channel-wise information from regions of interest.

4 Post-processing

A fundamental challenge in human pose estimation is that, the gap between *continuous joint space* and *discrete heatmap space* results in quantization error. Despite it is important for model performance, this error issue is largely ignored with little attention and efforts paid in most studies. To mitigate this problem, Newell et al. [52] presented a simple, heuristic method. Specifically, they shifted empirically the highest location \mathbf{m} in heatmap towards the second highest peak \mathbf{s} by a quarter of pixel to obtain the final output as:

$$\mathbf{p} = \mathbf{m} + 0.25 \frac{\mathbf{s} - \mathbf{m}}{\|\mathbf{s} - \mathbf{m}\|_2} \quad (3)$$

Since then, this ad-hoc method has been extensively used in the follow-up HPE models as *de-facto standard* post-processing. However, the rationale of this method is largely unknown. Importantly, how does this step affect the final model performance is under-studied.

To solve these issues, Zhang et al. [90] conducted a systematic investigation on post-processing. They revealed for the first time that this quantization error could introduce significant model performance degradation, particularly when low-resolution input images are used. Moreover, a superior distribution-aware post-processing method based on Taylor series approximation to Gaussian distribution was invented without re-training already-optimized HPE models. In particular, by approximating the heatmap distribution with Taylor series, it decodes human joint coordinates as:

$$\mathbf{p} = \mathbf{m} - (\mathcal{D}''(\mathbf{m}))^{-1} \mathcal{D}'(\mathbf{m}) \quad (4)$$

where the first- $\mathcal{D}'(\mathbf{m})$ and second-gradient $\mathcal{D}''(\mathbf{m})$ can be estimated efficiently around the outputted peak \mathbf{m} point only.

Subsequently, treating the predicted heatmap as a composite function of signal and noise, Yang et al. [84] proposed a Distribution-Aware and Error-Compensation (DAEC) decoding method to obtain coordinates of key-points by integrating over the entire heatmap. To achieve more accurate predictions, Fieraru et al. [29] proposed a data synthesis technique by simulating the typical erroneous samples and learning a pose refinement model from these synthesized samples to correct the predictions. Moon et al. [50] proposed a model-agnostic refinement method that adopts the diagnosis method [63] to analyze the common localization errors in HPE and utilizes the error statistics to synthesize new training samples. It is shown that a coarse-to-fine estimation network trained with these samples can improve effectively.

5 Supervision Representation

From the supervision representation perspective, HPE methods can be classified into *coordinate-based* [76, 26, 69] and *heatmap-based* methods [75, 60, 80, 46, 70]. Specifically, coordinate-based methods predict/regress the joint coordinates directly. Direct coordinate regression is intuitive and simple in model design. However, this approach often reaches only unsatisfactory model performance, largely due to that this regression learning task is extremely difficult particularly given unconstrained images.

On the other hand, the heatmap-based methods [75, 60, 80, 46, 70] take an extra advantage of the spatial structure information in the image to describe the relations between body parts and provide contextual and structural support for model learning. Usually these methods adopt discrete heatmaps to represent continuous distribution. The conversion from discrete heatmaps to coordinates is hence necessary which introduces quantization errors. To alleviate this problem, Sun et al. [72] treated the heatmap as an intermediate representation and proposed a differentiable integral approach to obtain the joint coordinate from the heatmap. Similar to [72], Nibali et al. [53] proposed a Differentiable Spatial to Numerical Transform (DSNT) method, as well as employed the Jensen-Shannon divergence to enforce a shape constraint on the distribution of heatmap. Besides, Earth Mover’s Distance (EMD) [49, 47] can also be utilized to measure the distribution between ground-truth and predicted heatmaps. Papandreou et al. [56] and Zhang et al. [93] explored an alternative to reduce the quantization error. They divided the localization

problem into two parts: a detection task and a regression task. The detection task learns binary heatmaps indicating the regions of body parts, whilst the regression task learns the fractional part of numerical joint coordinates. It is therefore a coarse-to-fine learning pipeline. To addressing significant model performance degradation from low-resolution, Wang et al. [13] introduced a novel Confidence-Aware Learning (CAL) method by addressing the fundamental training-testing discrepancy of previous offset learning methods [56, 93].

6 Human Pose Datasets

This section presents seven popular HPE datasets including BBC Pose datasets, ChaLearn dataset, Poses in the Wild dataset, Frames Labeled In Cinema datasets, Leeds Sports Pose datasets, MPII Human Pose dataset and Look Into Person dataset. Samples of each dataset are visualized in Fig. 2.

BBC Pose dataset. The BBC Pose dataset contains 20 videos extracted from BBC programmes, each of which is approximately 0.5h to 1.5h in length. There are 10/5/5 videos in the training set, validation set and test set respectively. There are 5 signers in the training and validation sets respectively, and 4 signers in the test set. Splitting the dataset this way aims to evaluate the generalization performance of HPE model in dealing with different signers. The annotation contains 7 joints, i.e., head, shoulders, elbows, wrists. The labels of training and validation sets are obtained by [7], while the samples in the test set are manually annotated. An extended version of this dataset, the extended BBC Pose dataset, includes additional 72 training videos annotated by the tracker of Charles et al. [11]. In addition, Charles et al. [11] also presented the Short BBC Pose dataset. This dataset contains 5 videos with different sleeve lengths compared to the BBC Pose and the extended BBC Pose datasets whose samples contain only long-sleeved signers. In order to evaluate the performance of algorithms on different videos accurately, each video contains 200 hand-annotated test frames and the final test set is composed of 5 videos.

ChaLearn dataset. The Chalearn dataset [25] is a multimodal dataset collected with the Kinect camera, including sound, 2D and 3D poses, RGB and depth images, and segmentation masks indicating regions of the human body from 27 persons. The dataset is split into 393/287/276 video clips for training, validation and testing, respectively. The whole human skeleton includes 20 joints, i.e., hip centre, spine, shoulder centre, head, shoulders, elbows, wrists, hands, hips, knees, feet,

ankles. The dramatic changes in clothing across videos cause the main challenge for HPE.

Poses in the Wild (PiW) dataset. To evaluate the performance of models in the wild, Cherian et al. [18] proposed the Poses in the Wild (PiW) dataset which consists of 30 sequences from 3 Hollywood movies. The PiW dataset defines 8 human upper-body keypoints (neck, shoulders, elbows, wrists, and mid-torso) and is characterized by occlusions, severe camera motion and background clutter.

Frames Labeled In Cinema (FLIC) dataset.

Similar to the PiW dataset, Frames Labeled In Cinema (FLIC) dataset [64] is extracted from 30 popular Hollywood movies and annotated by the crowdsourcing marketplace Amazon Mechanical Turk (AMT). The dataset has a total of 5003 images and is split into two parts: the training set (~80%, 3987 images) and the test set (~20%, 1016 images). Different from the PiW dataset with 8 keypoints, the annotation in FLIC dataset has 11 upper-body joints, namely nose, eyes, shoulders, elbows, wrists, and hips. The FLIC dataset has a full set version where all frames from movies are annotated by the AMT labelling service.

Leeds Sports Pose (LSP) dataset. In sports activities, there are many challenging cases such as motion blur, severe occlusion, extreme body deformation. The Leeds Sports Pose dataset [38] (LSP) is collected from Flickr to solve the pose estimation in sports activities. The dataset contains 2000 various sports images, with a half used for training and the other half for testing. Different from PiW and FLIC, LSP pays attention to the full-body pose estimation and defines the human pose with 14 joints, i.e., ankles, knees, hips, wrists, elbows, shoulders, neck, and head top.

MPII Human Pose (MHP) dataset. Deep learning based HPE methods require large amounts of data, but the sizes of early datasets are often limited. Small datasets cannot cover many practical cases and the lack of diversity could cause model overfitting particularly in deep learning. To address these issues, Andriluka et al. [2] established a taxonomy of daily activities and collected human images from various human activities in YouTube videos to build a large benchmark called MPII Human Pose (MHP) dataset. Compared with previous datasets, MHP dataset is characterized by its large scale and high diversity. The MHP dataset offers richer pose annotations including coordinates of 16 joints (i.e., shoulders, elbows, wrists, hips, knees, ankles, pelvis,

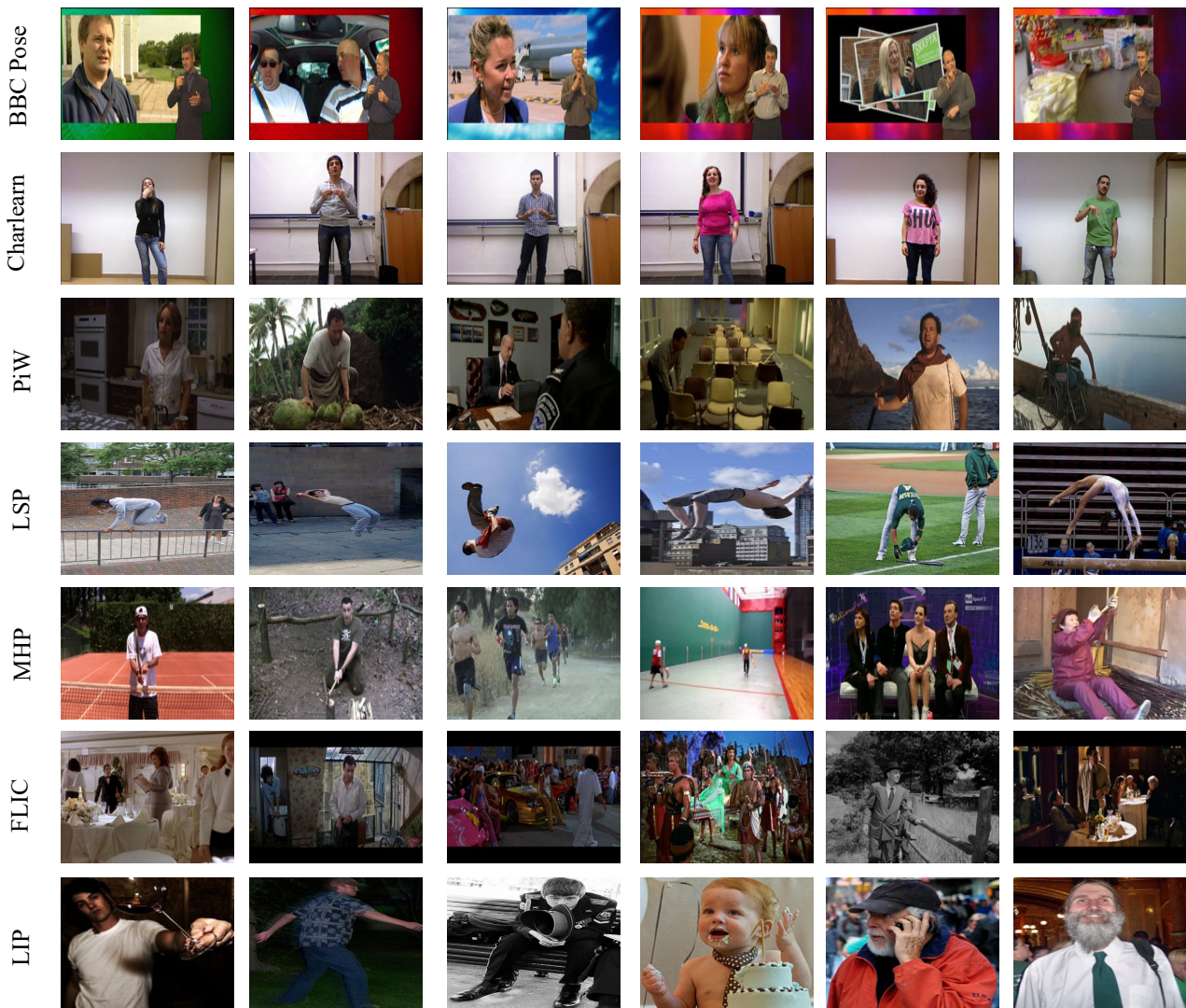


Fig. 2 Dataset samples. We show six random image samples for each dataset.

thorax, upper neck, head top), the corresponding visibility of these joints, 3D torso orientations, head orientations, and activity labels. This dataset is split into the train/valid/test sets of size 25863/2958/11701.

Look Into Person (LIP) dataset. Look Into Person (LIP) [42] is another large-scale and challenging dataset for human parsing and pose estimation. It contains 50,462 human images (19,081 full-body images, 13,672 upper-body images, 403 lower-body images, 3,386 head-missed images, 2,778 back-view images, and 21,028 images with occlusions) with challenging view, severe occlusions, various postures, varying clothing, and low resolution. This dataset is divided into 30,462 training images, 10,000 validation images and 10,000 test images. Each person is annotated with 16 joints (i.e.,

shoulders, elbows, wrists, hips, knees, ankles, head, neck, spine, and pelvis).

7 Performance Evaluation Metrics

This section focuses on the model evaluation metrics that differentiate the methods with some numerical index regarding their generalization performance.

Percentage of Correct Parts (PCP). Ferrari et al. [28] defined a performance criterion based on the stickmen annotation as shown in Fig. 3. In the definition of stickmen, each limb i of person n is simplified as a segment which has two endpoints $\{p_{i,1}^n, p_{i,2}^n\}$. When evaluating the Percentage of Correct Parts (PCP), the distance $d_{i,1}^n$ between the predicted joint $p_{i,1}^n$ and the

Table 2 Single person pose estimation datasets.

Dataset	Training/Val/Test	Parts	#Joints
BBC Pose [11]	10 videos/5 videos/5 videos	Upper body	7
Extended BBC Pose [11]	82 videos/5 videos/5 videos	Upper body	7
Short BBC Pose [11]	-/-/5 videos	Upper body	7
Charlearn [25]	393 videos/287 videos/276 videos	Full body	20
PiW [18]	total 30 videos	Upper body	8
FLIC [64]	3,987 images/-/1,016 images	Upper body	10
FLIC-full [64]	total 20928 images	Upper body	10
LSP [38]	1,000 images/-/1,000 images	Full body	14
Extended LSP [38]	11,000 images/-/1,000 images	Full body	14
MHP [2]	25,863 images/2,958 images/11,701 images	Full body	16
LIP [42]	30,462 images/10,000 images/10,000 images	Full body	16

**Fig. 3** The stickmen annotation. e_1^i and e_2^i are the two endpoints of limb i and l^i is the limb length, p_1^i and p_2^i are the corresponding predictions.

corresponding endpoint $e_{i,1}^n$ is normalized by the limb length $l_i^n = \|e_{i,1}^n - e_{i,2}^n\|_2$ formulated as:

$$d_{i,1}^n = \frac{\|p_{i,1}^n - e_{i,1}^n\|_2}{l_i^n} \quad (5)$$

Similarly, we can obtain another distance $d_{i,2}^n$:

$$d_{i,2}^n = \frac{\|p_{i,2}^n - e_{i,2}^n\|_2}{l_i^n} \quad (6)$$

The original PCP takes both endpoints into consideration. It calculates the distances from both endpoints to their corresponding predictions and then compares the average of both distances against a pre-set threshold to determine whether this limb is detected correctly:

$$\delta(i, n) = \begin{cases} 1, & \frac{d_{i,1}^n + d_{i,2}^n}{2} \leq r \\ 0, & \text{otherwise} \end{cases} \quad (7)$$

where r is the threshold and its value usually takes 50% of the limb length.

The original PCP for limb i is defined as:

$$\text{PCP}(i) = \sum_{n=1}^N \frac{\delta(i, n)}{N} \quad (8)$$

In addition to the original PCP metric, Johnson et al. [38] and Pishchulin et al. [61] adopted a stricter

$\delta(i, n)$ as:

$$\delta(i, n) = \begin{cases} 1, & d_{i,1}^n \leq r \text{ and } d_{i,2}^n \leq r \\ 0, & \text{otherwise} \end{cases} \quad (9)$$

Percent of Detected Joints (PDJ). Since the two PCP metrics penalize shorter limbs, they cannot reveal the actual performance of a HPE method. Toshev et al. [76] designed the Percent of Detected Joints (PDJ) which instead uses the torso diameter t^n as the scale factor to normalize the distance between the prediction p_j^n and the ground truth g_j^n for joint j of person n as:

$$d_j^n = \frac{\|p_j^n - g_j^n\|_2}{t^n} \quad (10)$$

Like the PCP metrics, if the normalized distance d_j^n is within a threshold r , the joint j of person n is considered detected. This can be formulated as:

$$\delta(j, n) = \begin{cases} 1, & d_j^n \leq r \\ 0, & \text{otherwise} \end{cases} \quad (11)$$

Thus, the PDJ for joint j can be defined as:

$$\text{PDJ}(j) = \sum_{n=1}^N \frac{\delta(j, n)}{N} \quad (12)$$

Percentage of Correct Keypoints (PCK). When evaluating the predictions of a model, the PDJ metric is greatly influenced by the torso diameter, making it less robust and consistent. Hence, Andriluka et al. [2] modified the PDJ metric by replacing the torso diameter with the head segment length h^n :

$$d_j^n = \frac{\|p_j^n - g_j^n\|_2}{h^n} \quad (13)$$

The resulting metric is named PCKh, defined as:

$$\text{PCKh}(j) = \sum_{n=1}^N \frac{\delta(d_j^n < 0.5)}{N} \quad (14)$$

Besides, they also computed the Area under the PCK Curve (AUC) with the threshold ranging from 0 to 0.5 for giving a more comprehensive evaluation.

Other Metrics. In addition to the above metrics, the researchers have also applied other metrics to assess the performance of a method from different perspectives. For example, the number of parameters is usually utilized to measure the model complexity and the Floating-point Operations (FLOPs) is adopted to evaluate the computing complexity [89]. The real-time performance is another key aspect for practical applications, and the Frames Per Second (FPS) is an often-used metric to evaluate the running speed at certain devices.

8 Conclusions and Discussions

This paper has reviewed a wide range of recent researches on HPE in the following four perspectives: data augmentation, model architecture, post-processing, and learning target. We discuss the development of HPE methods at data augmentation, model architecture, post-processing, and supervision representation. Although great improvements have been made, HPE still faces some fundamental challenges, as detailed below.

Transferability. Deep learning based HPE methods rely heavily on labelled data with specific characteristics. For example, the MHP dataset covers daily activities, while the LSP dataset focuses on the sports scene. The model trained on one dataset may perform badly on another dataset [12]. Thus, the transferability (i.e., model generalization across different domains) is still an important unsolved problem.

Severe occlusions. Occlusion resulting from varying shooting angles and crowd scenes remains a challenging problem in HPE. Some methods tackle this problem by learning explicit or implicit spatial models [80, 77], but suffer from the notorious overfitting issue. To deal with the occlusion problem efficiently and effectively, inferring the positions of occluded joints might give useful guidance information.

Low-resolution images. Low-resolution images are widely available in the wild and present extra challenges for state-of-the-art methods due to the lack of fine-grained appearance information. Nonetheless, it is still largely under-studied despite its potential importance in practice. There have been a couple of preliminary attempts on low-resolution challenge [51, 13] with more advanced models to be innovated in the future.

Real-time performance. Current researches mostly focus on designing deeper and more complicated HPE model to obtain higher accuracies. In many real-world applications, however, performing fast inference is likely a more important consideration especially for resource-limited platforms with human-computer interaction involved [89].

System integration and applications. The HPE is a fundamental task in computer vision with wide application values such as social robotics, human body generation, human-object interaction, activity recognition, person re-identification. Taking into account the integration of HPE in the whole system and conducting its research accordingly would be more focusing and purposing due to the presence of contextual knowledge and domain priors.

References

1. Andriluka M, Roth S, Schiele B (2009) Pictorial structures revisited: People detection and articulated pose estimation. In: 2009 IEEE conference on computer vision and pattern recognition, IEEE, pp 1014–1021
2. Andriluka M, Pishchulin L, Gehler P, Schiele B (2014) 2d human pose estimation: New benchmark and state of the art analysis. In: Proceedings of the IEEE Conference on Computer Vision and Pattern Recognition, pp 3686–3693
3. Artacho B, Savakis A (2020) Unipose: Unified human pose estimation in single images and videos. In: Proceedings of the IEEE/CVF Conference on Computer Vision and Pattern Recognition, pp 7035–7044
4. Baker B, Gupta O, Naik N, Raskar R (2016) Designing neural network architectures using reinforcement learning. arXiv preprint arXiv:161102167
5. Belagiannis V, Zisserman A (2017) Recurrent human pose estimation. In: 2017 12th IEEE International Conference on Automatic Face & Gesture Recognition (FG 2017), IEEE, pp 468–475
6. Bin Y, Cao X, Chen X, Ge Y, Tai Y, Wang C, Li J, Huang F, Gao C, Sang N (2020) Adversarial semantic data augmentation for human pose estimation. In: European conference on computer vision, pp 1–1
7. Buehler P, Everingham M, Huttenlocher DP, Zisserman A (2011) Upper body detection and tracking in extended signing sequences. *International journal of computer vision* 95(2):180

8. Bulat A, Tzimiropoulos G (2016) Human pose estimation via convolutional part heatmap regression. In: European Conference on Computer Vision, Springer, pp 717–732
9. Cao X, Ge Y, Tai Y, Zhang W, Li J, Wang C, Li J, Huang F (2019) Anti-confusing: Region-aware network for human pose estimation. arXiv preprint arXiv:190500996
10. Carreira J, Agrawal P, Fragkiadaki K, Malik J (2016) Human pose estimation with iterative error feedback. In: Proceedings of the IEEE conference on computer vision and pattern recognition, pp 4733–4742
11. Charles J, Pfister T, Everingham M, Zisserman A (2014) Automatic and efficient human pose estimation for sign language videos. *International Journal of Computer Vision* 110(1):70–90
12. Chen S, Zwicker M (2021) Transfer learning for pose estimation of illustrated characters. arXiv preprint arXiv:210801819
13. Chen W, Feng Z, Xiatian Z, Shuzhi SG (2021) Low-resolution human pose estimation. arXiv preprint arXiv:210909090
14. Chen X, Yuille AL (2014) Articulated pose estimation by a graphical model with image dependent pairwise relations. In: Advances in neural information processing systems, pp 1736–1744
15. Chen Y, Shen C, Wei XS, Liu L, Yang J (2017) Adversarial posenet: A structure-aware convolutional network for human pose estimation. In: Proceedings of the IEEE International Conference on Computer Vision, pp 1212–1221
16. Chen Y, Wang Z, Peng Y, Zhang Z, Yu G, Sun J (2018) Cascaded pyramid network for multi-person pose estimation. In: Proceedings of the IEEE conference on computer vision and pattern recognition, pp 7103–7112
17. Chen Y, Tian Y, He M (2020) Monocular human pose estimation: A survey of deep learning-based methods. *Computer Vision and Image Understanding* 192:102897
18. Cherian A, Mairal J, Alahari K, Schmid C (2014) Mixing body-part sequences for human pose estimation. In: Proceedings of the IEEE Conference on Computer Vision and Pattern Recognition, pp 2353–2360
19. Chou CJ, Chien JT, Chen HT (2018) Self adversarial training for human pose estimation. In: 2018 Asia-Pacific Signal and Information Processing Association Annual Summit and Conference (APSIPA ASC), IEEE, pp 17–30
20. Chu X, Ouyang W, Li H, Wang X (2016) Structured feature learning for pose estimation. In: Proceedings of the IEEE Conference on Computer Vision and Pattern Recognition, pp 4715–4723
21. Chu X, Ouyang W, Wang X, et al. (2016) Crf-cnn: Modeling structured information in human pose estimation. In: Advances in Neural Information Processing Systems, pp 316–324
22. Chu X, Yang W, Ouyang W, Ma C, Yuille AL, Wang X (2017) Multi-context attention for human pose estimation. In: Proceedings of the IEEE Conference on Computer Vision and Pattern Recognition, pp 1831–1840
23. Cireşan DC, Meier U, Gambardella LM, Schmidhuber J (2010) Deep, big, simple neural nets for handwritten digit recognition. *Neural computation* 22(12):3207–3220
24. Dang Q, Yin J, Wang B, Zheng W (2019) Deep learning based 2d human pose estimation: A survey. *Tsinghua Science and Technology* 24(6):663–676
25. Escalera S, González J, Baró X, Reyes M, Lopes O, Guyon I, Athitsos V, Escalante H (2013) Multimodal gesture recognition challenge 2013: Dataset and results. In: Proceedings of the 15th ACM on International conference on multimodal interaction, pp 445–452
26. Fan X, Zheng K, Lin Y, Wang S (2015) Combining local appearance and holistic view: Dual-source deep neural networks for human pose estimation. In: Proceedings of the IEEE conference on computer vision and pattern recognition, pp 1347–1355
27. Felzenszwalb PF, Huttenlocher DP (2005) Pictorial structures for object recognition. *International journal of computer vision* 61(1):55–79
28. Ferrari V, Marin-Jimenez M, Zisserman A (2008) Progressive search space reduction for human pose estimation. In: 2008 IEEE Conference on Computer Vision and Pattern Recognition, IEEE, pp 1–8
29. Fieraru M, Khoreva A, Pishchulin L, Schiele B (2018) Learning to refine human pose estimation. In: Proceedings of the IEEE conference on computer vision and pattern recognition workshops, pp 205–214
30. Fischler MA, Elschlager RA (1973) The representation and matching of pictorial structures. *IEEE Transactions on computers* 100(1):67–92
31. Gkioxari G, Toshev A, Jaitly N (2016) Chained predictions using convolutional neural networks. In: European Conference on Computer Vision, Springer, pp 728–743
32. Gong W, Zhang X, González J, Sobral A, Bouwmans T, Tu C, Zahzah Eh (2016) Human pose estimation from monocular images: A comprehensive survey. *Sensors* 16(12):1966

33. Gong X, Chen W, Jiang Y, Yuan Y, Liu X, Zhang Q, Li Y, Wang Z (2020) Autopose: Searching multi-scale branch aggregation for pose estimation. arXiv preprint arXiv:200807018
34. He K, Zhang X, Ren S, Sun J (2016) Deep residual learning for image recognition. In: Proceedings of the IEEE conference on computer vision and pattern recognition, pp 770–778
35. Hou L, Cao J, Zhao Y, Shen H, Meng Y, He R, Ye J (2020) Augmented parallel-pyramid net for attention guided pose-estimation. In: European conference on computer vision, pp 1–1
36. Jain A, Tompson J, Andriluka M, Taylor GW, Bregler C (2013) Learning human pose estimation features with convolutional networks. arXiv preprint arXiv:13127302
37. Ji X, Liu H (2009) Advances in view-invariant human motion analysis: a review. *IEEE Transactions on Systems, Man, and Cybernetics, Part C (Applications and Reviews)* 40(1):13–24
38. Johnson S, Everingham M (2010) Clustered pose and nonlinear appearance models for human pose estimation. In: *bmvc*, Citeseer, vol 2, p 5
39. Johnson S, Everingham M (2011) Learning effective human pose estimation from inaccurate annotation. In: *CVPR 2011*, IEEE, pp 1465–1472
40. Ke L, Chang MC, Qi H, Lyu S (2018) Multi-scale structure-aware network for human pose estimation. In: *Proceedings of the European Conference on Computer Vision (ECCV)*, pp 713–728
41. Krizhevsky A, Sutskever I, Hinton GE (2012) Imagenet classification with deep convolutional neural networks. In: *Advances in neural information processing systems*, pp 1097–1105
42. Liang X, Gong K, Shen X, Lin L (2018) Look into person: Joint body parsing & pose estimation network and a new benchmark. *IEEE transactions on pattern analysis and machine intelligence* 41(4):871–885
43. Lifshitz I, Fetaya E, Ullman S (2016) Human pose estimation using deep consensus voting. In: *European Conference on Computer Vision*, Springer, pp 246–260
44. Liu H, Simonyan K, Yang Y (2018) Darts: Differentiable architecture search. arXiv preprint arXiv:180609055
45. Liu H, Simonyan K, Yang Y (2019) DARTS: differentiable architecture search. In: *International conference on learning representations*, New Orleans, LA, USA
46. Liu W, Chen J, Li C, Qian C, Chu X, Hu X (2018) A cascaded inception of inception network with attention modulated feature fusion for human pose estimation. In: *Thirty-Second AAAI Conference on Artificial Intelligence*
47. Liu X, Maghlakelidze G, Zhou J, Izadi OH, Pommerenke D (2020) Detection of esd-induced soft failures by analyzing linux kernel function calls. *IEEE Transactions on Device and Materials Reliability* PP(99):1–1
48. Liu Z, Zhu J, Bu J, Chen C (2015) A survey of human pose estimation: the body parts parsing based methods. *Journal of Visual Communication and Image Representation* 32:10–19
49. Martin Arjovsky S, Bottou L (2017) Wasserstein generative adversarial networks. In: *Proceedings of the 34 th International Conference on Machine Learning*, Sydney, Australia
50. Moon G, Chang JY, Lee KM (2019) Posefix: Model-agnostic general human pose refinement network. In: *Proceedings of the IEEE Conference on Computer Vision and Pattern Recognition*, pp 7773–7781
51. Neumann L, Vedaldi A (2018) Tiny people pose. In: *Asian Conference on Computer Vision*, Springer, pp 558–574
52. Newell A, Yang K, Deng J (2016) Stacked hourglass networks for human pose estimation. In: *European conference on computer vision*, Springer, pp 483–499
53. Nibali A, He Z, Stuart M, Prendergast L (2018) Numerical coordinate regression with convolutional neural networks. *CoRR* abs/1801.07372
54. Nie X, Feng J, Zuo Y, Yan S (2018) Human pose estimation with parsing induced learner. In: *Proceedings of the IEEE Conference on Computer Vision and Pattern Recognition*, pp 2100–2108
55. Ning G, Zhang Z, He Z (2017) Knowledge-guided deep fractal neural networks for human pose estimation. *IEEE Transactions on Multimedia* 20(5):1246–1259
56. Papandreou G, Zhu T, Kanazawa N, Toshev A, Tompson J, Bregler C, Murphy K (2017) Towards accurate multi-person pose estimation in the wild. In: *Proceedings of the IEEE Conference on Computer Vision and Pattern Recognition*, pp 4903–4911
57. Park S, Lee Sb, Park J (2020) Data augmentation method for improving the accuracy of human pose estimation with cropped images. *Pattern Recognition Letters* 136:244–250
58. Peng X, Tang Z, Yang F, Feris RS, Metaxas D (2018) Jointly optimize data augmentation and network training: Adversarial data augmentation in human pose estimation. In: *Proceedings of the IEEE Conference on Computer Vision and Pattern*

- Recognition, pp 2226–2234
59. Pfister T, Simonyan K, Charles J, Zisserman A (2014) Deep convolutional neural networks for efficient pose estimation in gesture videos. In: Asian Conference on Computer Vision, Springer, pp 538–552
 60. Pfister T, Charles J, Zisserman A (2015) Flowing convnets for human pose estimation in videos. In: Proceedings of the IEEE International Conference on Computer Vision, pp 1913–1921
 61. Pishchulin L, Jain A, Andriluka M, Thormählen T, Schiele B (2012) Articulated people detection and pose estimation: Reshaping the future. In: 2012 IEEE Conference on Computer Vision and Pattern Recognition, IEEE, pp 3178–3185
 62. Rafi U, Leibe B, Gall J, Kostrikov I (2016) An efficient convolutional network for human pose estimation. In: BMVC, vol 1, p 2
 63. Ruggero Ronchi M, Perona P (2017) Benchmarking and error diagnosis in multi-instance pose estimation. In: Proceedings of the IEEE international conference on computer vision, pp 369–378
 64. Sapp B, Taskar B (2013) Modec: Multimodal decomposable models for human pose estimation. In: Proceedings of the IEEE Conference on Computer Vision and Pattern Recognition, pp 3674–3681
 65. Sarafianos N, Boteanu B, Ionescu B, Kakadiaris IA (2016) 3d human pose estimation: A review of the literature and analysis of covariates. *Computer Vision and Image Understanding* 152:1–20
 66. Saxena S, Verbeek J (2016) Convolutional neural fabrics. In: Advances in Neural Information Processing Systems, pp 4053–4061
 67. Simonyan K, Zisserman A (2014) Very deep convolutional networks for large-scale image recognition. arXiv preprint arXiv:1409.1556
 68. Su K, Yu D, Xu Z, Geng X, Wang C (2019) Multi-person pose estimation with enhanced channel-wise and spatial information. In: Proceedings of the IEEE Conference on Computer Vision and Pattern Recognition, pp 5674–5682
 69. Sun K, Lan C, Xing J, Zeng W, Liu D, Wang J (2017) Human pose estimation using global and local normalization. In: Proceedings of the IEEE International Conference on Computer Vision, pp 5599–5607
 70. Sun K, Xiao B, Liu D, Wang J (2019) Deep high-resolution representation learning for human pose estimation. In: Proceedings of the IEEE conference on computer vision and pattern recognition, pp 5693–5703
 71. Sun X, Shang J, Liang S, Wei Y (2017) Compositional human pose regression. In: Proceedings of the IEEE International Conference on Computer Vision, pp 2602–2611
 72. Sun X, Xiao B, Wei F, Liang S, Wei Y (2018) Integral human pose regression. In: Proceedings of the European Conference on Computer Vision (ECCV), pp 529–545
 73. Tang W, Wu Y (2019) Does learning specific features for related parts help human pose estimation? In: Proceedings of the IEEE Conference on Computer Vision and Pattern Recognition, pp 1107–1116
 74. Tompson J, Goroshin R, Jain A, LeCun Y, Bregler C (2015) Efficient object localization using convolutional networks. In: Proceedings of the IEEE conference on computer vision and pattern recognition, pp 648–656
 75. Tompson JJ, Jain A, LeCun Y, Bregler C (2014) Joint training of a convolutional network and a graphical model for human pose estimation. In: Advances in neural information processing systems, pp 1799–1807
 76. Toshev A, Szegedy C (2014) Deeppose: Human pose estimation via deep neural networks. In: Proceedings of the IEEE conference on computer vision and pattern recognition, pp 1653–1660
 77. Wang J, Long X, Gao Y, Ding E, Wen S (2020) Graph-pcnn: Two stage human pose estimation with graph pose refinement. In: European Conference on Computer Vision, Springer, pp 492–508
 78. Wang P, Li W, Ogunbona P, Wan J, Escalera S (2018) Rgb-d-based human motion recognition with deep learning: A survey. *Computer Vision and Image Understanding* 171:118–139
 79. Wang Z, Li W, Yin B, Peng Q, Xiao T, Du Y, Li Z, Zhang X, Yu G, Sun J (2018) Mscoco keypoints challenge 2018. In: Joint Recognition Challenge Workshop at ECCV 2018, vol 5
 80. Wei SE, Ramakrishna V, Kanade T, Sheikh Y (2016) Convolutional pose machines. In: Proceedings of the IEEE conference on Computer Vision and Pattern Recognition, pp 4724–4732
 81. Xia F, Wang P, Chen X, Yuille AL (2017) Joint multi-person pose estimation and semantic part segmentation. In: Proceedings of the IEEE Conference on Computer Vision and Pattern Recognition, pp 6769–6778
 82. Xiao B, Wu H, Wei Y (2018) Simple baselines for human pose estimation and tracking. In: Proceedings of the European conference on computer vision (ECCV), pp 466–481
 83. Xu C, Yu X, Wang Z, Ou L (2020) Multi-view human pose estimation in human-robot interaction. In: IECON 2020 The 46th Annual Conference of

- the IEEE Industrial Electronics Society, IEEE, pp 4769–4775
84. Yang F, Chen Y, Pan Z, Zhang M, Xue M, Mo Y, Zhang Y, Guan G, Qian B, Xiao Z, et al. (2020) Train your data processor: Distribution-aware and error-compensation coordinate decoding for human pose estimation. arXiv preprint arXiv:200705887
 85. Yang S, Yang W, Cui Z (2019) Pose neural fabrics search. arXiv preprint arXiv:190907068
 86. Yang W, Ouyang W, Li H, Wang X (2016) End-to-end learning of deformable mixture of parts and deep convolutional neural networks for human pose estimation. In: Proceedings of the IEEE Conference on Computer Vision and Pattern Recognition, pp 3073–3082
 87. Yang W, Li S, Ouyang W, Li H, Wang X (2017) Learning feature pyramids for human pose estimation. In: proceedings of the IEEE international conference on computer vision, pp 1281–1290
 88. Yang Y, Ramanan D (2011) Articulated pose estimation with flexible mixtures-of-parts. In: CVPR 2011, IEEE, pp 1385–1392
 89. Zhang F, Zhu X, Ye M (2019) Fast human pose estimation. In: Proceedings of the IEEE/CVF Conference on Computer Vision and Pattern Recognition, pp 3517–3526
 90. Zhang F, Zhu X, Dai H, Ye M, Zhu C (2020) Distribution-aware coordinate representation for human pose estimation. In: Proceedings of the IEEE/CVF Conference on Computer Vision and Pattern Recognition, pp 7093–7102
 91. Zhang H, Ouyang H, Liu S, Qi X, Shen X, Yang R, Jia J (2019) Human pose estimation with spatial contextual information. arXiv preprint arXiv:190101760
 92. Zhang P, Lan C, Xing J, Zeng W, Xue J, Zheng N (2019) View adaptive neural networks for high performance skeleton-based human action recognition. *IEEE transactions on pattern analysis and machine intelligence* 41(8):1963–1978
 93. Zhang R, Zhu Z, Li P, Wu R, Guo C, Huang G, Xia H (2019) Exploiting offset-guided network for pose estimation and tracking. In: Proceedings of the IEEE/CVF Conference on Computer Vision and Pattern Recognition (CVPR) Workshops
 94. Zheng L, Huang Y, Lu H, Yang Y (2019) Pose-invariant embedding for deep person re-identification. *IEEE Transactions on Image Processing* 28(9):4500–4509
 95. Zoph B, Le QV (2016) Neural architecture search with reinforcement learning. arXiv preprint arXiv:161101578